J. Fluid Mech. (1995), *vol.* 287, *pp.* 1–20

The occurrence of moist 'anticonvection' in a water–air system

By OLEG V. PERESTENKO AND LEV KH. INGEL

Institute of Experimental Meteorology, SPA 'Typhoon', 82 Lenin Avenue, Obninsk, Kaluga Region 249020, Russia

(Received 6 September 1993 and in revised form 7 October 1994)

A non-Rayleigh mechanism of instability in horizontally homogeneous hydrodynamic systems consisting of two immiscible fluids and heated uniformly from above, i.e. 'anticonvection', was first investigated theoretically by Welander (1964) and more recently (and independently) by Gershuni & Zhukhovitsky (1980). This paper discusses the possibility of 'anticonvection' occurring in a water–air system, taking into account evaporation, stratification with respect to moisture, thermocapillary effects and the presence of a surface heat source at the water–air interface. For this purpose, a linear problem of stability is solved, in which the Rayleigh number analogues in each of the fluids are its eigenvalues in one case and the increments of disturbances in the other. It has been shown that taking into account evaporation and stratification with respect to moisture in the air reveals a new feedback in the system resulting in the disappearance of one of the previously known areas of anticonvection and the formation of new areas of instability. The mechanism of the oscillatory regime of the loss of stability in the system under study was found and considered in detail. Increments and wavelengths of the growing modes are calculated, and the possibility of experimental investigation of moist anticonvection in laboratory and field conditions is discussed.

1. Introduction

The term 'anticonvection' was coined by Welander (1964) to describe a new non-Rayleigh mechanism of convective instability. From a linear analysis of instability he obtained a theoretical result that might appear at first sight to be paradoxical: the state of mechanical equilibrium of a horizontally homogeneous system consisting of two immiscible fluids heated from above (stably stratified) may be unstable, followed by the development of convection in both fluids near the interface.

More recently a theoretical work by Gershuni & Zhukhovitsky (1980) was published, in which the authors considered independently a similar problem on the stability of equilibrium in a system consisting of two layers of immiscible fluids of finite depth heated from above. This work supports the results of Welander on the possibility of instability of this type. Both works mentioned above analyse a physical mechanism of anticonvection, which differs essentially from the Rayleigh one in its nature. It can be briefly explained as follows.

Let us assume, for example, that as a result of a random disturbance, an element of the upper (lighter) fluid has shifted downwards in the direction of the interface. In its new position, this element is at a higher temperature than its surroundings, since it has come from a higher and warmer region, closer to the source of heat input into the system from above. If the upper fluid has relatively small temperature conductivity and

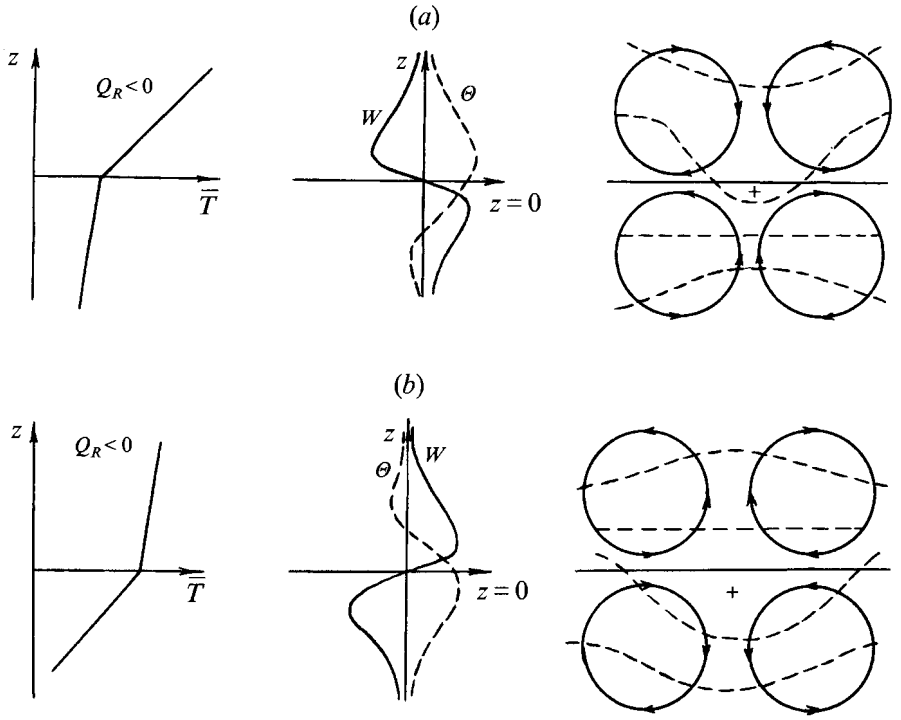

FIGURE 1. A schematic of vertical profiles of the background temperature ($\bar{T}$), disturbances of temperature and vertical velocity (Θ and W), and streamlines (solid curves) and isotherms (dashed curves) in convective cells for anticonvection of (*a*) the divergent and (*b*) convergent types.

thermal expansion, the element will cool down rather slowly, having in the process a relatively small buoyancy. However, owing to heat exchange through the interface, the heat lost by the element and conducted through the interface results in some fluid below having a higher temperature than other fluid at the same level (figure 1 *a*). If thermal expansion in the lower fluid is rather large, the heated element in it will be distinctly lighter than its surroundings. When floating up to the surface, it will spread beneath the interface. Owing to the continuity of shearing stress, spreading will be induced over the interface in the upper fluid as well. From continuity considerations, this implies an enhancement of downward motions in the upper fluid, i.e. strengthening of the initial disturbance. Thus, in the two-layer system there is a positive feedback which in favourable cases may lead to a spontaneous development of disturbances under the condition of stable stratification of both fluids. By convention, we arbitrarily call the disturbances developing in the above situation anticonvection of divergent type (a divergence of streamlines at the interface corresponds to positive values of temperature disturbances).

In works by Perestenko & Ingel (1989, 1991) a more general situation is considered, when the presence of a surface heat source (sink) is assumed at the interface. It has been shown theoretically that for any pair of interacting fluids, depending on the value of the intensity Q of this source (sink), both the divergent and convergent types of anticonvection can be realized. In particular, at sufficiently large positive values of Q, when stratification in the lower fluid is sufficiently stable whereas in the upper one it is close to neutral, remaining stable, the convergent type of anticonvection is realized (see figure 1 *b*). Otherwise, when the heat sink is sufficiently intensive (see figure 1 *a*), the

conditions for the occurrence of anticonvection of the divergent type can always be created.

In Welander (1964) and Gershuni & Zhukhovitsky (1980), the possibility of observing anticonvection under laboratory conditions is discussed. However, an attempt to demonstrate this type of instability in a mercury–water system (see Welander 1971) has been unsuccessful, and at the present time no successful experiments on anticonvection have come to our notice. As may be inferred from the Welander (1971) and G. P. Bogatyrev (1992, personal communication), the causes of failure of experimental studies of anticonvection is most likely the following. Since a certain amount of dissolved oxygen from the air is always present in the water, a stiff oxide film is formed at the mercury surface which is in contact with the water. This film inhibits the dynamic interaction between the fluids necessary for instability. Another possible cause of failure is insufficient purity of water and mercury, giving admixtures which are also capable of forming films at the interface which hinder the transfer of tangential stresses from one fluid to another. More recently, some other theoretical works taking into account additional contributory factors from experimental observation on anticonvection in the fluid–fluid system have also been published. For instance, Nepomnyaschy & Simanovsky (1990) allowed for the effect of heat release at the interface on the occurrence of convection in a system heated from above and consisting of two fluids of finite depth. This work discussed the situation in which temperature gradients in both fluids may be opposite in direction as a result of heat release at the interface. This enabled an investigation of the interaction of Rayleigh- and Welander-type instabilities. The combined effect of Welander-type thermocapillary instabilities was investigated in a recent work by Perestenko (1992). He showed that taking into account a 'normal' temperature dependence of the interfacial tension allows one to extend substantially the area of instability for anticonvection of the divergent type. Some results relative to anticonvection are also presented in Gershuni, Zhukhovitsky & Simanovsky (1981) and Gershuni, Zhukhovitsky & Pershina (1983), the former work, in particular, containing numerical investigations of finite-amplitude motions in two-layer systems heated from above.

Bearing in the mind possible geophysical applications and the above-mentioned difficulties of laboratory modelling of anticonvection in a liquid–liquid system, in the present work the stability of the interaction of laminar layers of water and moist air is investigated within the framework of the classical linear analysis in the absence of base flows and with stable density stratification in each layer. In earlier work we have already started investigating anticonvection, as applied to the problem of large-scale interaction of the ocean and atmosphere (Perestenko & Ingel 1989, 1991; Ingel & Perestenko 1992, 1994). In the present work, attention is focused, for the first time, on the study of the roles of the process of evaporation from the water surface and stratification with respect to the air moisture in the occurrence of anticonvection in a water–air system.

The paper is organized as follows: §2 describes the setting up of a linear stability problem for a water–air system and formulates the boundary conditions for the background state and for disturbances. In §3, the characteristic equation of the problem is written and some of its asymptotics are found. A regime is discovered in which neutral oscillations occur in the water–air system. Based on simple physical considerations, the mechanism of these oscillations is discussed, and an analytical expression for their frequency is derived. In the general case, a number of numerical solutions of the characteristic equation are presented as neutral curves determining the boundaries of instability areas. In §4, the growth rates and wavelengths of unstable

disturbances are investigated, and an analytical relation between them in the long-wave limit is found. In conclusion (§5) the results obtained are summarized, and their applicability to field conditions and the possibility of experimental observations of moist anticonvection are discussed.

2. Setting up the problem

2.1. *Mechanical equilibrium*

Let us consider a system which consists of two horizontally homogeneous stably stratified fluids, semi-infinite in the vertical direction, and in mechanical equilibrium (figure 2). We position the Cartesian axes in such a way that $z = 0$ corresponds to the interface, a positive axis to moist air, and a negative axis to water. Denoting the equilibrium distributions of density, temperature, specific humidity (mixing ratio) and pressure by $\bar{\rho}$, $\bar{T}$, $\bar{q}$ and $\bar{p}$, respectively, and assuming that the air is unsaturated everywhere, except the interface, we obtain the equation for mechanical equilibrium in each of the fluids in the Boussinesq approximation:

$$\nabla \bar{P}_i + \bar{\rho}_i g \boldsymbol{e}_z = 0, \tag{2.1}$$

$$\nabla^2 \bar{T}_i = 0, \tag{2.2}$$

$$\nabla^2 \bar{q} = 0, \tag{2.3}$$

$$\bar{\rho}_1 = \rho_{0_1}[1 - \alpha_1(\bar{T}_1 - \bar{T}_0) - \delta(\bar{q} - \bar{q}^*(\bar{T}_0))], \tag{2.4}$$

$$\bar{\rho}_2 = \rho_{0_2}[1 - \alpha_2(\bar{T}_2 - \bar{T}_0)] \quad (i = 1, 2). \tag{2.5}$$

Here $\delta = m_a/m_w - 1$, m_a and m_w being the molar masses of dry air and water, respectively, α_i is the thermal expansion coefficient, ρ_{0_i} is the average value of density, $\boldsymbol{e}_z$ is the unit vector along the z-axis, and ∇ is the Hamiltonian operator. Hereafter we shall denote by subscripts 1 and 2 the parameters and variables relating to the upper and lower fluid, respectively. At the interface ($z = 0$), the following conditions should be met:

$$\bar{P}_1 = \bar{P}_2, \quad \bar{T}_1 = \bar{T}_2 \equiv \bar{T}_0, \quad \bar{q} = \bar{q}^*(\bar{T}_0). \tag{2.6}$$

The last condition in (2.6) implies the fulfilment of the condition of air saturation immediately above the water surface. From (2.2), (2.3) and conditions (2.6) it follows that

$$\bar{T}_1 = \bar{T}_0 + \gamma_i z, \tag{2.7}$$

$$\bar{q} = \bar{q}^*(\bar{T}_0) + \gamma_q z, \tag{2.8}$$

Here $\gamma_i = \partial_z \bar{T}_i \geqslant 0$ and $\gamma_q = \partial_z \bar{q} \leqslant 0$ are the vertical gradients of temperature and specific humidity, indicating a linear increase of temperature with height in both fluids and a linear decrease of specific humidity with height in moist air (figure 2). In this paper we shall restrict our consideration to those situations where the density in both fluids does not increase (as a rule, it decreases) with height. In particular, for the upper fluid it implies the fulfilment of the following inequality:

$$\frac{1}{\rho_{0_1}} \partial_z \bar{\rho}_1 = -\alpha_1 \gamma_1 - \delta \gamma_q \leqslant 0.$$

Now we supplement the conditions (2.6) with the heat balance equation describing the latent–sensible flux relation at the interface:

$$\rho_{0_2} C_{p_2} \kappa_2 \gamma_2 = \rho_{0_1} C_{p_1} \kappa_1 \gamma_1 + \rho_{0_1} D L_v \gamma_q + Q_R, \tag{2.9}$$

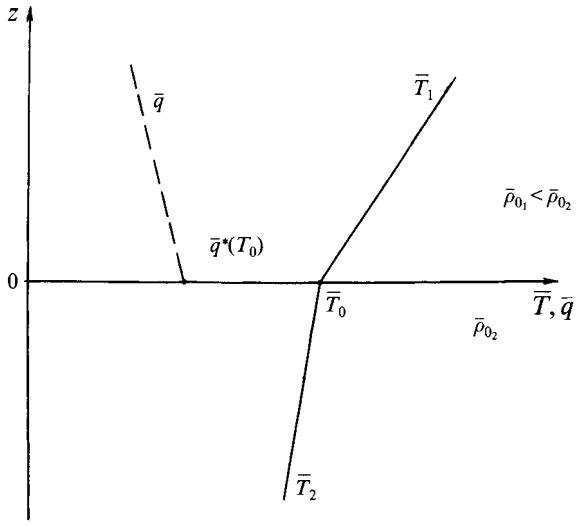

FIGURE 2. A schematic of vertical profiles of the background temperature ($\bar{T}$) and specific moisture ($\bar{q}$) for the problem of moist anticonvection.

where C_{p_i} is the specific heat capacity at constant pressure, κ_i and D are the coefficients of thermal conductivity and water vapour diffusion, respectively, L_v is the latent heat of vaporization, and Q_R is the intensity of the surface heat source (sink) which in geophysical applications is determined by the radiation balance of the water–air interface. Next we set $\kappa_i = D$ because their values are close to each other.

2.2. *Boundary-value problem for disturbances*

Assuming that ρ_i, T_i, q and P_i are the disturbances to the equilibrium state of a two-layer system heated from above, we can write the linear equations for disturbances in the Boussinesq approximation for each of the fluids:

$$(\partial_t - \nu_i \nabla^2)\, \boldsymbol{v}_i = -\frac{\nabla}{\rho_{0_i}} P_i - g\frac{\rho_i}{\rho_{0_i}} \boldsymbol{e}_z, \tag{2.10}$$

$$(\partial_t - \kappa_i \nabla^2)\, T_i + \gamma_i \boldsymbol{v}_i \cdot \boldsymbol{e}_z = 0, \tag{2.11}$$

$$(\partial_t - \kappa_1 \nabla^2)\, q + \gamma_q \boldsymbol{v}_1 \cdot \boldsymbol{e}_z = 0, \tag{2.12}$$

$$\nabla \cdot \boldsymbol{v}_i = 0, \tag{2.13}$$

$$\rho_1/\rho_{0_1} = -(\alpha_1 T_1 + \delta q) = -\alpha_1 T_v, \tag{2.14}$$

$$\rho_2/\rho_{0_2} = -\alpha_2 T_2. \tag{2.15}$$

Here $\boldsymbol{v}_i$ is the three-dimensional vector of a disturbance velocity field, ν_i is the kinematic viscosity coefficient, and $T_v = T_1 + (\delta/\alpha_1) q$ is the virtual air temperature. We now state a set of boundary conditions.

We assume that far from the interface (at $|z| \to \infty$) all disturbances are damped out. In this case, it remains to determine the disturbance interfacial conditions. Deformations of the interface are neglected (Welander 1964; Ingel & Perestenko 1992). Furthermore, disturbances of horizontal components of the velocity and temperature fields are taken to be continuous at $z = 0$, whereas tangential stresses at the interface undergo a discontinuity caused by the presence of a thermocapillary effect. A further condition may be obtained if we write the thermal balance equation at the interface

(2.9) for disturbances of the latent and sensible heat fluxes, assuming that there are no disturbances of the intensity of the surface heat source (sink) Q_R. Thus, at $z = 0$ we can write

$$\left.\begin{gathered} W_1 = W_2 = 0, \quad \boldsymbol{u}_1 = \boldsymbol{u}_2, \\ \rho_{0_1}\nu_1\partial_z\boldsymbol{u}_1 - \sigma_T\nabla_h T_2 = \rho_{0_2}\nu_2\partial_z\boldsymbol{u}_2, \quad T_1 = T_2 \equiv T_0, \\ \rho_{0_1}C_{p_1}\kappa_1\partial_z T_1 + \rho_{0_1}\kappa_1 L_v\partial_z q = \rho_{0_2}C_{p_2}\kappa_2\partial_z T_2, \\ \nabla_h = \nabla_h(\partial_x, \partial_y), \end{gathered}\right\} \tag{2.16}$$

where $\boldsymbol{u}_i$ is the vector of horizontal components of the velocity field and W_i is the vertical component. The parameter $\sigma_T = \partial\sigma/\partial T$ characterizes a 'normal' temperature dependence of the surface tension coefficient (Gershuni & Zhukhovitsky 1972):

$$\sigma = \sigma_0 - \sigma_T T_0. \tag{2.17}$$

It should be noted that the set of boundary conditions (2.16) is incomplete, since it does not contain an expression for the disturbance of the saturation specific humidity q^* at the interface. This quantity is uniquely determined by the water surface temperature. For small disturbances q^* is proportional to the disturbance of the water surface temperature T_0. From the standard relations of moist air thermohydrodynamics and the Clausius–Clapeyron equation in the Boussinesq approximation one can derive (Perestenko 1993):

$$q^* = \left(\frac{\bar{q}^* L_v}{R_v \bar{T}_0^2}\right) T_0, \tag{2.18}$$

where R_v is the gas constant for water vapour. Thus, the set of equations (2.10)–(2.15) and the set of boundary conditions (2.16) and (2.18) state the boundary-value problem for the equilibrium-state disturbances.

3. Linear analysis of stability

3.1. *The equation and interfacial conditions for the vertical velocity*

We seek a solution of the set of equations (2.10)–(2.15) in the form of normal disturbances:

$$(\boldsymbol{v}_i, T_i, q, T_v, p_i) = \{V_i(z), \Theta_i(z), \hat{q}(z), \Theta_v(z), P_i(z)\}\exp[\omega t + \mathrm{i}(k_x x + k_y y)]. \tag{3.1}$$

Here $\omega = \omega_r + \mathrm{i}\omega_i$ is the complex increment of disturbances; k_x and k_y are the wavenumbers characterizing the periodicity of disturbances along the x- and y-directions, respectively; $V_i(z)$, $\Theta_i(z)$, $\hat{q}(z)$, $\Theta_v(z)$, and $P_i(z)$ are the complex amplitudes of disturbances. It is evident that at $\omega_r = 0$ the system will be in the neutral state, which will determine its stability limits. Substituting (3.1) into (2.10)–(2.15) reduces this set of equations to a single ordinary linear homogeneous differential equation with respect to the amplitude of the vertical velocity $W_i(\zeta)$ in each of the fluids:

$$\{(\mathrm{d}^2_{\zeta\zeta} - \lambda^2_{1i})(\mathrm{d}^2_{\zeta\zeta} - \lambda^2_{2i})(\mathrm{d}^2_{\zeta\zeta} - 1) - R_i\}\, W_i(\zeta) = 0. \tag{3.2}$$

Here, similarly to Welander (1964) and Ingel & Perestenko (1992), we introduce the following notation: $\zeta = kz$ is the dimensionless vertical coordinate ($k^2 = k_x^2 + k_y^2 = (2\pi/L)^2$); $R_i = N_i^2/(\kappa_i\nu_i k^4)$ is the analogue of the Rayleigh number in each fluid; $\lambda^2_{1i} - 1 = \lambda^2_{0i} = \omega/\nu_i k^2$ and $\lambda^2_{2i} - 1 = \lambda^2_{0i} Pr_i$ are the dimensionless 'viscous' and 'diffusion' time scales of the problem. Here $N_1^2 = \alpha_1\gamma_1(1-\phi)g$ and $N_2^2 = \alpha_2\gamma_2 g$ are the buoyancy frequencies squared in the upper and lower fluid, respectively, $\varphi = -\delta\gamma_q/$

$\alpha_1 \gamma_1$ is the density ratio in the moist air (a dimensionless parameter determining the stratification in the upper fluid), and $Pr_i = \nu_i/\kappa_i$ is the Prandtl number in each of the fluids. It should be noted that the requirement on stability of the background density stratification (in the limiting case, of the neutral one) in the upper fluid determines the variation range of the dimensionless parameter φ from zero (neutral stratification with respect to moisture) to unity (neutral density stratification), whereas for stratification in water it is necessary that $\gamma_2 \geqslant 0$.

It can easily be shown that the set of boundary conditions (2.16), and (2.18) can be reduced to

$$W_1 = W_2 = 0, \tag{3.3}$$

$$\mathrm{d}_\zeta W_1 = \mathrm{d}_\zeta W_2, \tag{3.4}$$

$$\epsilon_1 \mathrm{d}^2_{\zeta\zeta} W_1 = \frac{Mr}{R_2}(\mathrm{d}^2_{\zeta\zeta} - \lambda^2_{12})(\mathrm{d}^2_{\zeta\zeta} - 1) W_2 + \mathrm{d}^2_{\zeta\zeta} W_2, \tag{3.5}$$

$$\epsilon_2 \left(\frac{\epsilon_q}{1+\epsilon_q}\right)(\mathrm{d}^2_{\zeta\zeta} - \lambda^2_{11})(\mathrm{d}^2_{\zeta\zeta} - 1) W_1 = (\mathrm{d}_{\zeta\zeta} - \lambda^2_{12})(\mathrm{d}^2_{\zeta\zeta} - 1) W_2, \tag{3.6}$$

$$\epsilon_3 \left(\frac{1-\epsilon_L \varphi}{1-\epsilon_L}\right)(\mathrm{d}^2_{\zeta\zeta} - \lambda^2_{11})(\mathrm{d}^2_{\zeta\zeta} - 1)\left[\mathrm{d}_\zeta - \lambda_{21}\left(\frac{1-\epsilon_L}{1-\epsilon_L \varphi}\right)\left(\frac{1+\epsilon_q \varphi}{1+\epsilon_q}\right)\right] W_1$$
$$= (\mathrm{d}^2_{\zeta\zeta} - \lambda^2_{12})(\mathrm{d}^2_{\zeta\zeta} - 1)\mathrm{d}_\zeta W_2. \tag{3.7}$$

Here, similarly to Welander (1964), we introduce the following dimensionless parameters:

$$\epsilon_1 = \frac{\rho_{0_1} \nu_1}{\rho_{0_2} \nu_2}; \quad \epsilon_2 = \frac{\nu_1 \alpha_2}{\nu_2 \alpha_1}; \quad \epsilon_3 = \frac{\rho_{0_1} C_{p_1} \kappa_1}{\rho_{0_2} C_{p_2} \kappa_2} \epsilon_2; \quad \epsilon_L = \frac{\alpha_1 L_v}{\delta C_{p_1}}; \quad \epsilon_q = \frac{R_v \bar{T}_{0_1}}{\delta \bar{q}^* L_v}.$$

Taking into account the thermocapillary effects at the interface in (3.5) leads to the appearance of an analogue of the thermal Marangoni number for water $Mr = (\sigma_T \gamma_2)/(\rho_{0_2} \kappa_2 \nu_2 k^2)$. Thus, the problem of stability, completely formulated mathematically, incorporates equation (3.2), the interfacial conditions at $\zeta = 0$ (3.3)–(3.7) and the requirement $W_i \to 0$ at $|\zeta| \to \infty$.

3.2. *Characteristic equation of the problem*

The solution of equation (3.2) can be written as

$$W_i(\zeta) = \sum_{n=1}^{6} C_{ni} \exp(r_{ni} \zeta). \tag{3.8}$$

Here the r_{ni} are the roots of the equation

$$(r_i^2 - \lambda^2_{1i})(r_i^2 - \lambda^2_{2i})(r_i^2 - 1) - R_i = 0. \tag{3.9}$$

Equation (3.9) has six roots r_{ni} with $\mathrm{Re}(r_{1i}, r_{2i}, r_{3i}) \geqslant 0$, whereas $r_{4i} = -r_{1i}; r_{5i} = -r_{2i}$; and $r_{6i} = -r_{3i}$. Consequently, to fulfil the condition of damping of all disturbances far from the interface in the expression for W_1, only the exponents with roots $-r_{11}$, $-r_{21}$, and $-r_{31}$ should remain, whereas in the expression for W_2 those with roots r_{12}, r_{22}, and r_{32} should be left. For the remaining six arbitrary constants $C_{ni} (n = 1, 2, 3; i = 1, 2)$ we have from the interfacial conditions (3.3)–(3.7) six algebraic equations which enable us to write the following characteristic equation:

$$F(R_i, Mr, \lambda_{1i}, \lambda_{2i}, \epsilon_1, \epsilon_2, \epsilon_3, \epsilon_q, \epsilon_L, \varphi) = \det(A_{i,j}) = 0, \tag{3.10}$$

where $A_{i,j}$ is a complex 6×6 matrix, the elements of which are presented in explicit form Perestenko (1993). It is easy to show that a limiting transition takes place from this stability problem to the Welander (1964) problem for two fluids when evaporation and thermocapillary effects are ignored.

3.3. *Some asymptotics*

In view of the cumbersomeness of the matrix $A_{i,j}$ in equation (3.10) and the presence of radicals r_{ni} which are the roots of the bicubic equation (3.9) with complex coefficients, the stability analysis of the system under consideration, in full and without resorting to numerical techniques, is fairly complicated. However, some asymptotics can be analysed quite easily.

Thus in Welander (1964) and Perestenko & Ingel (1991) two asymptotic limits for 'dry' anticonvection were analysed: a 'long-wave' limit ($k\to 0$, $R_1, R_2\to\infty$) and a 'short-wave' one ($k\to\infty$, R_1, $R_2\to 0$). In these works it was shown that in the short-wave limit, without considering thermocapillary effects, a two-layer system is always stable, whereas in the long-wave limit all modes grow with a wavelength greater than the critical one, provided that the instability criterion found is satisfied. It was also found that in the presence of sufficiently intensive surface heat sources (sinks) Q_R in two-layer fluids, it is possible that there exist two areas of instability for any pair of fluids for all cases. A divergent type of anticonvection (the ratio γ_1/γ_2 is sufficiently great) corresponds to the case of an intensive heat source $Q_R > 0$, whereas a convergent type (γ_1/γ_2 is sufficiently small) corresponds to the case of a heat sink $Q_R < 0$.

Let us consider long-wave asymptotics, when we may neglect the horizontal exchange and thermocapillary effects, and use the hydrostatics approximation. The combined effect of Welander-type and 'thermocapillary' instabilities (with Sternling & Scriven 1959 being the first to study the latter) was investigated without considering evaporation in a recent paper by Perestenko (1992). The short-wave limit was also analytically investigated in that paper.

First we assume that $\omega_r = \omega_i = 0$, which corresponds to mechanical equilibrium. Equation (3.10) at $\varphi \neq 1$ in the long-wave limit ($k\to 0$, $R_1, R_2\to\infty$) takes the form

$$\hat{\epsilon}_2\hat{\epsilon}_3\hat{\epsilon}_4 - 4\epsilon_1\hat{\epsilon}_3\hat{\epsilon}_4^{2/3}(1-\tfrac{3}{2}\mu) - 3\epsilon_1\hat{\epsilon}_2\hat{\epsilon}_4^{1/2} + \epsilon_1 - 4\hat{\epsilon}_2\hat{\epsilon}_4^{1/3} - 3\hat{\epsilon}_3\hat{\epsilon}_4^{1/2}(1-2\mu) = 0, \quad (3.11)$$

where

$$\left.\begin{aligned} &\hat{\epsilon}_2 = \epsilon_2\left(\frac{\epsilon_q}{1+\epsilon_q}\right), \quad \hat{\epsilon}_3 = \epsilon_3\left(\frac{1-\epsilon_L\varphi}{1-\varphi}\right), \quad \hat{\epsilon}_4 = \epsilon_4(1-\varphi) = \frac{R_1}{R_2}, \\ &\mu = \left(\frac{1+\epsilon_q\varphi}{1+\epsilon_q}\right)\left(\frac{1-\epsilon_L}{1-\epsilon_L\varphi}\right)R_1^{-1/6}, \quad \epsilon_4 = \frac{\alpha_1\gamma_1\kappa_2\nu_2}{\alpha_2\gamma_2\kappa_1\nu_1} = \frac{Ra_1}{R_2}, \quad Ra_1 = \frac{\alpha_1\gamma_1 g}{\kappa_1\nu_1 k^4}. \end{aligned}\right\} \quad (3.12)$$

Note that for the upper fluid we introduced two analogues of the Rayleigh number: a 'density' (R_1) and a 'thermal' (Ra_1) one. In equation (3.11) the external parameters of the problem are γ_1, γ_2 and φ, whereas the dimensionless parameter μ is small and may be neglected everywhere, except for the limit $\varphi\to 1/\epsilon_L$. Let us consider (3.11) as an algebraic equation with respect to $\epsilon_4 = Ra_1/R_2$ with a variable parameter φ. Using the Cartesian theorem of the number of positive roots of a polynomial and finding their approximate values, we can draw inferences about the number of instability areas of the given system and the position of neutral curves. The dependence of the roots of equation (3.11) on the value of the external parameter φ at $\bar{T}_0 = 293$ K, which was found numerically, is plotted in figure 3. It is seen from this figure and an approximate

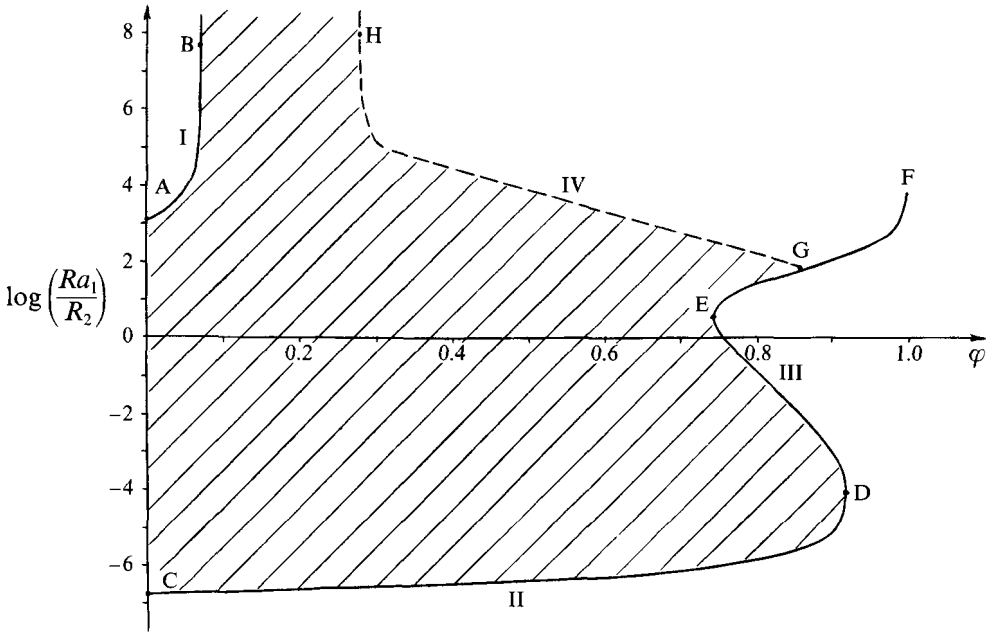

FIGURE 3. Neutral curves on the plane of parameters $(\log(Ra_1/R_2), \varphi)$ in the limit $Ra_1^{1/3}, R_2^{1/3} \gg 1$. The solid line represents the stability boundaries for monotonic modes, and the dashed line for oscillating ones. The stable area is hatched.

analysis of (3.11) that the entire variation range of the parameter φ can be divided into three subranges.

(i) $0 < \varphi < 1/\epsilon_L$. Here there are two roots:

$$(Ra_1/R_2)_1 \approx (4/\hat{\epsilon}_3)^{3/2}(1-\varphi)^{-1}, \tag{3.13}$$

$$(Ra_1/R_2)_2 \approx (\epsilon_1/4\hat{\epsilon}_2)^3(1-\varphi)^{-1}. \tag{3.14}$$

Their values determine the position in figure 3 of neutral curves AB and CD, respectively, which bound two instability areas in this subrange, where the situation coincides qualitatively with the results obtained by Perestenko & Ingel (1991) for 'dry' anticonvection. The areas I and II correspond to anticonvection of divergent and convergent types respectively.

Further, with growing φ (as $|\gamma_q|$ increases at fixed γ_1), instability area II expands slightly, while area I shrinks drastically and in the limit $\varphi \to 1/\epsilon_L$ ($\hat{\epsilon}_3 \to 0$ and $(Ra_1/R_2)_1 \to \infty$) vanishes. In other words, an increase of stratification with respect to moisture and of evaporation leads to suppression of anticonvection of the divergent type. Let us explain this in greater detail. The air volume shifting downwards to the interface turns out to be warmer and drier than its surroundings. In this case, the water volume in contact with it is simultaneously heated due to contact heat exchange and cooled because of enhanced evaporation. To maintain a positive feedback, it is necessary for this cooling to be weaker than the heating, i.e. the Bowen ratio for the disturbances, which is determined as the ratio of disturbed fluxes of sensible and latent heat, should satisfy the following inequality:

$$Bo_p = \frac{C_{p_1}\partial_z \Theta_1}{L_v \partial_z q} < -1.$$

It can be shown that this ratio in the long-wave limit practically coincides with the Bowen ratio for base fluxes

$$Bo_p \approx Bo_f = \frac{\rho_{0_1} C_{p_1} \kappa_1 \gamma_1}{\rho_{0_1} L_v \kappa_1 \gamma_q} = \frac{C_{p_1} \delta}{L_v \alpha_1} \left(\frac{\alpha_1 \gamma_1}{\delta \gamma_q} \right) = -\frac{1}{\epsilon_L \varphi}. \tag{3.15}$$

Thus, in the limit $\varphi \to 1/\epsilon_L$ (Bo_p, $Bo_f \to -1$) the above-mentioned heating and cooling effects compensate each other, with the result that the temperature of the water volume under the interface remains virtually constant. This leads to suppression of the positive feedback necessary for the occurrence of anticonvection of the divergent type and to stabilization of the system.

(ii) $1/\epsilon_L < \varphi < (\epsilon_3 + \frac{4}{3})/(\epsilon_3 \epsilon_L + \frac{4}{3})$. In this subrange, only one root $(Ra_1/R_2)_2$ remains, which bounds the instability area of the convergent type II.

(iii) $(\epsilon_3 + \frac{4}{3})/(\epsilon_3 \epsilon_L + \frac{4}{3}) \leqslant \varphi < 1$. At $\varphi \approx (\epsilon_3 + \frac{4}{3})/(\epsilon_3 \epsilon_L + \frac{4}{3})$, in addition to the root $(Ra_1/R_2)_2$, one more root of equation (3.11) appears (point E in figure 3). It can be written approximately as

$$(Ra_1/R_2)_3 \approx (-4\hat{\epsilon}_2/3\hat{\epsilon}_3)^6 (1-\varphi)^{-1}. \tag{3.16a}$$

The appearance of this root implies that there is a new instability area (area III in figure 3) in the subrange under consideration, which owes its origin entirely to the enhanced role of evaporation in the system under study with increasing φ. The position of branch EF of the neutral curve bounding area III from above is given by

$$(Ra_1/R_2)_4 \approx (3/\hat{\epsilon}_2)^2 (1-\varphi)^{-1}, \tag{3.16b}$$

whereas the position of branch ED of the neutral curve bounding area III from below until it merges with area II at point D is approximately given by (3.16*a*). A physical mechanism for the instability arising in the area III is as follows. Ascending motions over the water surface in moist air lead to a decrease of the total vertical gradients of temperature and moisture, and consequently to a reduction of the absolute values of latent and sensible heat fluxes at the interface. In the vicinity of point E in figure 3 $\varphi \approx 0.75$, Bo_p and $Bo_f \approx -0.1$. This implies that the predominant effect of ascending motions in the air is a substantial reduction of evaporation from the water surface and the occurrence of a positive disturbance of temperature at the interface. This thermal disturbance leads to enhancement of the initial ascending motions in the air and to further development of instability.

Thus, in the system under consideration there is a previously unknown instability area III which owes its origin entirely to the above-mentioned positive convection–evaporation feedback and is possible only at sufficiently small values of Bo_p and Bo_f. It should be noted here that the flow arising in the lower fluid plays a stabilizing role in the case under study, tending to impose descending motions on the upper fluid. This enables one to assume that such a mechanism of stability loss can be realized more effectively above a well-moistened solid surface (Perestenko & Ingel 1993). In conclusion, it should be emphasized that in the limit $\varphi \to 1$ the system turns out to be unstable to monotonic disturbances at any stable thermal stratifications of both fluids.

3.4. *Anticonvective oscillations*

Along with instability of the monotonic type, the analysis of the water–air system under consideration also revealed an oscillatory regime of stability loss (corresponding to $\omega_i \neq 0$). Its boundary in the long-wave limit is plotted in figure 3 as the curve GH calculated numerically from equation (3.10). The simplest way to analyse the occurrence of oscillations in the system and understand their mechanism is to consider the case where stratification of the lower fluid is rather weak, whereas the upper one

is stratified sufficiently stably. These conditions imply the fulfilment of the following inequalities:

$$|\lambda_{11}^2|, |\lambda_{21}^2| \ll R_1^{1/3}, \quad |\lambda_{12}^2|, |\lambda_{22}^2| \gg R_2^{1/3}, \quad R_1/R_2 \to \infty. \tag{3.17a–c}$$

In this case we are able to expand analytically a determinant in (3.10) and reduce it to two algebraic equations in φ and ω_i by setting the real and imaginary parts equal to zero. The roots of these equations determine the position of the stability boundary and the neutral oscillation frequency ω_i. Thus, taking into account (3.17*a–c*), we can obtain from (3.10) the following expression for the stability boundary:

$$\varphi_{min} \approx \frac{\epsilon_3 + b}{\epsilon_3 \epsilon_L + b}, \tag{3.18}$$

where

$$b = \frac{3\epsilon_1 \hat{\epsilon}_2 Pr_2^{1/2}}{1 + 4\epsilon_1 (2 Pr_2^{1/2}(1 + Pr_2^{1/2})/(3\epsilon_1 \hat{\epsilon}_2))^{1/4}}.$$

Expression (3.18) determines the minimum allowable value of φ in the given system at which neutral oscillations are possible. It is easily seen from figure 3 that the neutral curve GH approaches the value φ_{min} at $(Ra_1/R_2) \sim 10^6$. Similarly, we can obtain from (3.10) and (3.17*a–c*) the following expression for ω_i:

$$(\lambda_{02}^2/R_1^{1/3}) \approx (2\sqrt{2}\,\epsilon_1 \hat{\epsilon}_3/(\hat{\epsilon}_3 + 3\epsilon_1 \hat{\epsilon}_2 Pr_2^{1/2}))^2, \tag{3.19}$$

which may be approximated, in view of (3.18), by

$$\omega_i \approx \left(\frac{\rho_{0_1} \alpha_2 g L_v |\gamma_q| (1 + Bo_f)}{\rho_{0_2} C_{p_2} 2(1 + Pr_2^{1/2})}\right)^{1/2} (\kappa_1 \nu_1)^{1/6} (N_1/k^2)^{-1/3}. \tag{3.20}$$

Notice that the necessary condition for the existence of neutral oscillations $Bo_f > -1$ (or $\varphi > 1/\epsilon_L$) follows immediately from (3.20), whereas the sufficient condition is given by (3.18).

It can be shown that an expression of the type (3.20) can be easily obtained solely from simple physical considerations explaining the nature of the anticonvective oscillations revealed here.

Let us assume that the temperature disturbance variations at the interface follow the law

$$\Theta_1(\zeta = 0) = \Theta_2(\zeta = 0) = \Theta_0 \sin(kx) \sin(\omega_i t), \tag{3.21}$$

where, for definiteness, $\Theta_0 > 0$. Then the depth to which the thermal disturbance penetrates into the lower fluid is $H_2 \sim H_{\kappa_2}$, where $H_{\kappa_2} = (\kappa_2/\omega_i)^{1/2}$ is the vertical 'diffusive' scale in this fluid. This follows immediately from (3.17*b*) if we rewrite it as

$$H_{R_2} \gg H_{\kappa_2}, H_{\nu_2}, \tag{3.22}$$

where $H_{\nu_2} = (\nu_2/\omega_i)^{1/2}$ and $H_{R_2} = (\nu_2 \kappa_2/N_2^2 k^2)^{1/6}$ are vertical 'diffusive' and 'density' scales. Next, assuming that $H_2 \ll k^{-1}$ (a long-wave approximation), we may neglect the horizontal exchange and use the hydrostatics approximation. Then it is easy to estimate the horizontal pressure gradients originating in a layer of thickness H_2:

$$|P_2| \sim g|\rho_2| H_2 = g\rho_{0_2} \alpha_2 H_2 \Theta_0, \quad |\partial_x P_2/\rho_{0_2}| \sim g\alpha_2 H_2 \Theta_0 k. \tag{3.23}$$

Hereafter, for brevity, we omit factors of the type $\sin(kx)\sin(\omega_i t)$.

The horizontal pressure gradients cause the corresponding flows in the lower fluid. Thus, in the area where $\Theta_2 > 0$, there is a spreading under the interface, and ascending motions occur. Here we can estimate the characteristic horizontal velocity from the balance of forces of baric gradient and viscosity in the horizontal motion equation. We obtain

$$|U_2| \sim \frac{H_{\nu_2}^2}{\nu_2 \rho_{0_2}} |\partial_x P_2| \approx \frac{g\alpha_2 H_2 \Theta_0 k}{\omega_i}. \tag{3.24}$$

Because of the continuity of tangential stresses at the interface, the lower fluid sets the upper one in motion. Therefore in the lower air layer of thickness H_1, there are also horizontal flows with the characteristic absolute value of velocity $|U_1| \sim |U_2|$. The depth of this layer is determined by density stratification, which is evident from the condition (3.17*a*) written as

$$H_{R_1} \ll H_{\kappa_1}, H_{\nu_1}, \tag{3.25}$$

where H_{κ_1}, H_{ν_1} and H_{R_1} are the diffusive, viscous and density scales in the upper fluid, respectively. Consequently, it should be assumed that $H_1 \sim H_{R_1}$, from whence and the continuity equation we obtain the characteristic absolute value of vertical velocity in the upper fluid:

$$|W_1| \sim kH_{R_1}|U_1| \sim \frac{g\alpha_2 H_2 H_1 \Theta_0 k^2}{\omega_i}. \tag{3.26}$$

It is easy to see that in this case, over the more heated area of the water surface in the upper fluid descending flows occur together with spreading above the interface, which are imposed by motions in the lower fluid. The descending motions carry dryer and warmer air from above to the water surface. We can assess these disturbances in moisture and temperature by approximately equating the terms $W_1\gamma_q$ and $\kappa_1\partial^2_{zz}q$, $W_1\gamma_1$ and $\kappa_1\partial^2_{zz}\Theta_1$, respectively, in the transfer equations (2.11) and (2.12). Whence it follows that

$$|q| \sim \frac{|\gamma_q| H^2_{R_1}}{\kappa_1} W_1 \sim \frac{g\alpha_2 |\gamma_q| H_2 H_1^3 \Theta_0 k^2}{\kappa_1 \omega_i}, \tag{3.27a}$$

$$|\Theta_0| \sim \frac{\gamma_1 H^2_{R_1}}{\kappa_1} W_1 \sim \frac{g\alpha_2 \gamma_1 H_2 H_1^3 \Theta_0 k^2}{\kappa_1 \omega_i}. \tag{3.27b}$$

Drying the air over the water surface leads to enhanced evaporation and therefore a disturbance of the latent heat flux,

$$\rho_{0_1}\kappa_1 L_v |\partial_z q| \sim \rho_{0_1} L_v g\alpha_2 |\gamma_q| H_2 H_1^2 \Theta_0 k^2/\omega_i. \tag{3.28a}$$

Simultaneously, the sensible heat flux in the air directed toward the water is disturbed as well,

$$\rho_{0_1} C_{p_1}\kappa_1 |\partial_z \Theta_1| \sim \rho_{0_1} C_{p_1} g\alpha_2 \gamma_1 H_2 H_1^2 \Theta_0 k^2/\omega_i. \tag{3.28b}$$

The absolute value of the heat flux disturbance in the lower fluid can be written as

$$\rho_{0_2} C_{p_2}\kappa_2 |\partial_z \Theta_2| \sim \rho_{0_2} C_{p_2}\kappa_2 \Delta\Theta_2/H_2, \tag{3.28c}$$

where $\Delta\Theta_2$ is the absolute value of the characteristic vertical decrease of the temperature disturbance in the water layer of thickness H_2. If the ratio $\rho_{0_1}\kappa_1 L_v|\partial_z q|/\rho_{0_1} C_{p_1}\kappa_1|\partial_z\Theta_1| = |1/Bo_f| > 1$, a water layer of thickness about H_2 will be cooled. This cooling will continue until the water surface cools down to about Θ_0. In turn, this will lead to the occurrence of a descending motion and a horizontal convergence of flows in the water, and a process similar to the one above will develop, but of opposite sign for all disturbances (the second half-period of oscillation). The values of $\Delta\Theta_2$ and Θ_0 are of the same order of magnitude. In fact, as cooling of the surface due to evaporation dominates over its heating owing to contact heat exchange ($|Bo_f| < 1$), and the temperature disturbance at $\zeta = 0$ becomes negative, a positive deviation of temperature of approximately Θ_0 still persists at a depth of about H_2. This is easily seen from a direct analysis of the vertical temperature profiles (Perestenko 1993) as well. Taking into account the fact that the fluxes of latent and sensible heat are oppositely directed ($Bo_f < 0$), we substitute the expressions for the fluxes (3.28*a–c*) into the heat balance

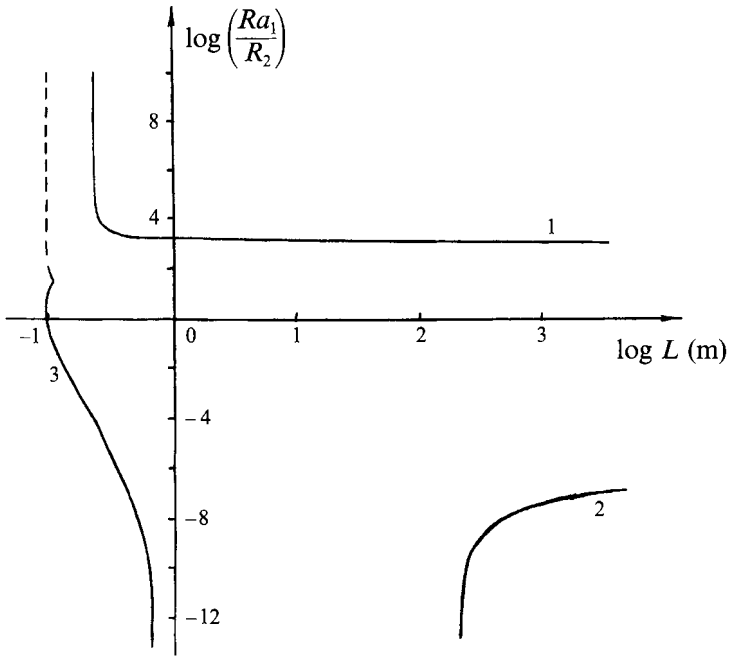

FIGURE 4. A set of neutral curves on the plane $(\log(Ra_1/R_2), \log L)$ at $\sigma_T = 0.144 \times 10^{-3}$ N m^{-1} K^{-1} and $\varphi = 0$ (curves 1 and 2) and $\varphi = 1.0$ (curve 3). Solid lines represent portions of the stability boundaries for monotonic modes, and dashed lines for oscillating ones.

equation from (2.16). Assuming that $\Delta\Theta_2 \sim \Theta_0$ and substituting the appropriate expressions for H_1 and H_2, we obtain an expression for the oscillation frequency of the system which is similar to (3.20):

$$\omega_i \sim \left(\frac{\rho_{0_1}\alpha_2 g L_v |\gamma_q|(1+Bo_f)}{\rho_{0_2} C_{p_2}}\right)^{1/2} (\kappa_1 \nu_1)^{1/6} (N_1/k^2)^{-1/3}. \tag{3.29}$$

The above considerations contain a number of simplifications but can be substantiated more fully and tested *a posteriori*.

From the analysis of the disturbance profiles in both fluids (Perestenko 1993) it may be concluded that thermal disturbances at the interface determine the dynamics in the lower fluid which in turn imposes a corresponding circulation on the upper fluid. Further, vertical motions in the upper fluid control the fluxes of latent and sensible heat at the water–air interface and so determine the thermal disturbances at the interface. This corresponds to the scheme of fluid interaction considered above.

The fact that from simple physical considerations one can reproduce the expression for the neutral oscillation frequency supports the correctness of our understanding of the mechanism of anticonvective oscillations.

3.5. *Results of numerical calculations of neutral curves*

In this section we consider the numerical solutions of equation (3.10) without any restrictions on the wavelengths of the modes under study. Figure 4 shows the neutral curves for the monotonic and oscillatory types of instability plotted in the plane of the parameters of the problem $(\log(Ra_1/R_2), \log(L))$ at various values of φ. These curves determine the position of the stability boundaries of the system. From the foregoing asymptotic analysis (see figure 3) it follows that at $\varphi = 0$ (dry anticonvection) there are

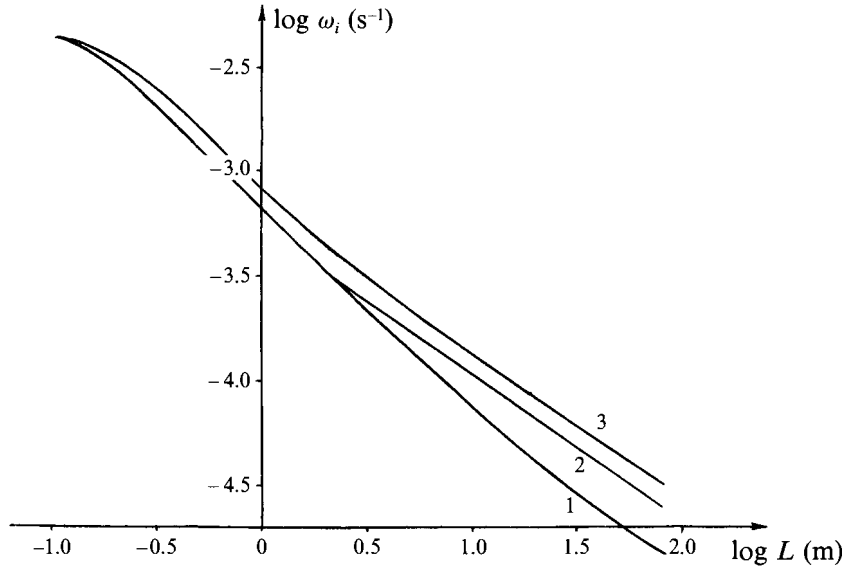

FIGURE 5. Dispersion curves for neutral oscillating modes on the plane ($\log\omega_i$, $\log L$) at $\sigma_T = 0.144 \times 10^{-3}$ N m^{-1} K^{-1} and $\log(Ra_1/R_2) \to \infty$ (curve 1); $\log(Ra_1/R_2) = 4$ (curve 2); and $\log(Ra_1/R_2) = 2$ (curve 3).

two instability areas, located above curve 1 and below curve 2, respectively. In the limit of large L ($Ra_1^{1/3}$, $R_2^{1/3} \gg 1$) curves 1 and 2 approach the values of the ratio (Ra_1/R_2) following from expressions (3.13) and (3.14), respectively. Convergent instability (its area is bounded by curve 2) on the interval of small L is suppressed by thermocapillary effects. In the limit $\log(Ra_1/R_2) \to -\infty$ curve 2 asymptotically approaches the vertical line that corresponds to the value of L following from an approximate equality of the form:

$$\frac{Mr\, R_1^{1/3}}{R_2} \approx \frac{\epsilon_1}{2\hat{\epsilon}_2}. \tag{3.30}$$

It should be noted that the asymptotics (3.30) is true in this limit for all neutral curves for which $0 < \varphi < 1.0$. In the opposite limit $\log(Ra_1/R_2) \to \infty$ curve 1 is given by $R_1^{2/3} \approx 16/\epsilon_3$. In the limiting case $\varphi = 1.0$ a unified instability area is located to the right of the neutral curve 3 consisting of two portions. The first is the stability boundary for monotonic disturbances (solid line) and occurs at $\log(Ra_1/R_2) \leqslant 1.5$, whereas the second separates the damped oscillations from the growing ones (dashed line) and appears at $\log(Ra_1/R_2) \geqslant 1.5$. In the limit $\log(Ra_1/R_2) \to -\infty$ curve 3 approaches the vertical line that corresponds to the value of L following from the approximate equality

$$\frac{R_2}{Mr} \approx \frac{4\hat{\epsilon}_2}{\epsilon_1}. \tag{3.31}$$

From the position of the neutral curve 3 it appears that as the ratio (Ra_1/R_2) decreases, the instability area on the interval of small L is reduced under the influence of thermocapillary effects. The dispersion curves calculated numerically from equation (3.10) and fitting the positions of the stability boundaries at different values of the ratio (Ra_1/R_2) are plotted in figure 5 on the plane of parameters $(\log\omega_i, \log L)$. In the limit of large L each of these curves develops a dependence of the form $\omega_i \sim L^{-2/3}$ or $\omega_i \sim k^{2/3}$, obtained previously analytically in the expressions (3.20) and (3.29).

4. Growth rates of disturbances

As well as the stability boundaries of the system, we investigated growth rates of disturbances. In terms of the prospects for experimental studies on this instability and its investigation in field conditions, of particular interest is the study of growth rates in those situations most favourable for its development. This applies to the case where the lower fluid is neutrally stratified ($R_2 = 0$), and in the upper fluid a stable temperature gradient is compensated for by an unstable humidity gradient, so that the density stratification is neutral ($\varphi \to 1$, $R_1 \to 0$). Then some of the negative feedback in the system is absent, since instability energy is not expended as work against buoyancy forces in each of the fluids. Besides, in this case question (3.10) is simplified, and its analysis enables one to find the long-wave asymptotics ($Ra_i^{1/3}, \lambda_{0_i} \gg 1$; $i = 1, 2$) for the increment:

$$\omega_r \approx \left(\frac{\kappa_1^{3/2} \rho_{0_1} L_v \alpha_1 g |\gamma_q| (1 + \epsilon_q)}{2\kappa_2^{1/2} \rho_{0_2} C_{p_2} \epsilon_q (1 + Pr_1^{1/2})} k^2 \right)^{1/3}. \tag{4.1}$$

The two-thirds power law $\omega_r \sim L^{-2/3}$ at $L \geqslant 1$ m is clearly seen in figure 6 which presents a numerical solution of equation (3.10) with and without consideration of thermocapillary effects. Next, as in §3.4, let us show that an expression for ω_r similar to (4.1) can be readily obtained from simple physical considerations.

We assume that at the interface the temperature inhomogeneity which is periodic in the horizontal direction and exponentially growing with time is given by

$$\Theta_1(\zeta = 0) = \Theta_2(\zeta = 0) = \Theta_0 \cos(kx) \exp(\omega_r t), \tag{4.2}$$

where the amplitude $\Theta_0 > 0$. Let us denote the height to which the temperature disturbance penetrates into the upper fluid by H_1. Assuming that $H_1 \ll k^{-1}$, we use the hydrostatics approximation and neglect the horizontal exchange. Then it is easy to evaluate the pressure disturbance:

$$|P_1| \sim g |\rho_1| H_1 \approx g \rho_{0_1} \alpha_1 H_1 \Theta_0; \quad |\partial_x P_1 / \rho_{0_1}| \sim g \alpha_1 H_1 \Theta_0 k \tag{4.3}$$

(for brevity, we omit factors of the type $\cos(kx) \exp(\omega_r t)$). Next, we assume that in the linearized equation of horizontal motion the terms $\partial_t U_1$ and $\partial_x P_1 / \rho_{0_1}$ are of the same order of magnitude. Hence, taking into account (4.3), the characteristic value of the horizontal velocity in the upper fluid can be written as

$$|U_1| \sim g \alpha_1 H_1 \Theta_0 k / \omega_r. \tag{4.4}$$

Further, from continuity considerations,

$$|W_1| \sim H_1 k |U_1| \sim \frac{g \alpha_1 \Theta_0 H_1^2 k^2}{\omega_r}. \tag{4.5}$$

Vertical motions lead to disturbances in the humidity field. The amplitude of these disturbances can be evaluated from the equation

$$\partial_t q - \kappa_1 \partial_{zz}^2 q \approx -\gamma_q W_1. \tag{4.6}$$

It is easy to verify that both terms on the left-hand side of (4.6) are of the same order of magnitude, therefore either of them may be equated in order of magnitude to the right-hand side. Hence

$$|q| \sim |\gamma_q W_1| / \omega_r \sim g \alpha_1 |\gamma_q| H_1^2 \Theta_0 k^2 / \omega_r^2. \tag{4.7}$$

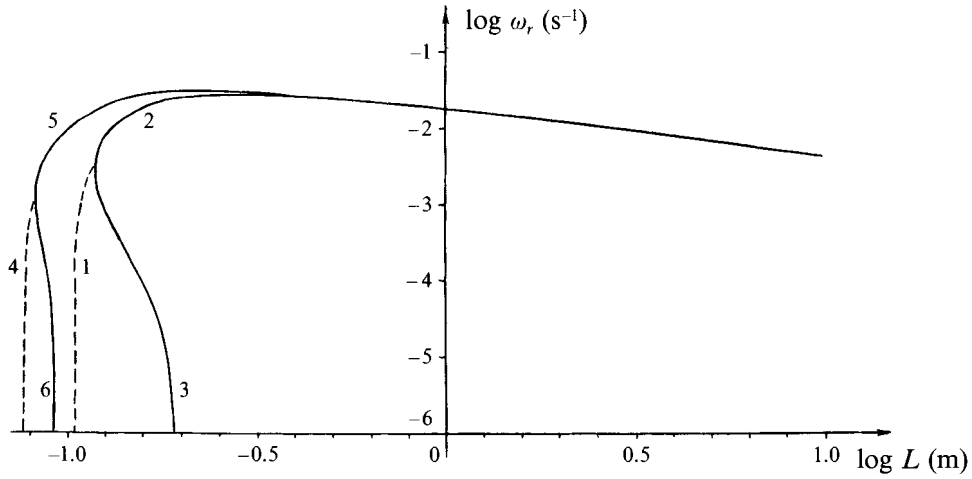

FIGURE 6. Increments of growing modes on the plane ($\log\omega_r$, $\log L$) in the case $\log(Ra_1/R_2)\to\infty$ at $\varphi = 1.0$ and $\sigma_T = 0.144\times10^{-3}$ N m^{-1} K^{-1} (curves 1, 2 and 3); and $\sigma_T = 0$ (curves 4, 5 and 6). The dashed lines 1 and 4 represent the real parts of the pairs of complex increments.

Since there are descending motions over the colder portions of the interface, they carry drier air from above. In its turn, this leads to an enhanced evaporation in this portion, i.e. to an additional flux of latent heat

$$\kappa_1 L_v \rho_{0_1} |\partial_z q| \sim \kappa_1 L_v \rho_{0_1} |q|/H_1 \sim g\alpha_1 \kappa_1 L_v \rho_{0_1} |\gamma_q| H_1 \Theta_0 k^2/\omega_r^2. \tag{4.8}$$

The relations between densities, specific heat capacities and exchange coefficients in two fluids are such that, as is easy to verify, evaporation is mainly accounted for by cooling of the lower fluid. Thus, (4.8) should be approximately equated to the absolute value of heat flux from the lower fluid,

$$\rho_{0_2} C_{p_2} \kappa_2 |\partial_z \Theta_2| \sim \rho_{0_2} C_{p_2} \kappa_2 \Delta\Theta_2/H_2, \tag{4.9}$$

where H_2 is the effective depth of a layer of the lower fluid cooled upon additional evaporation, and $\Delta\Theta_2$ is the characteristic absolute value of this cooling. The meaning of latter value is the same as that of the temperature disturbance amplitude Θ_0 introduced above. By equating $|\Delta\Theta_2|$ and $|\Theta_2|$ in order of magnitude, with allowance made for an approximate equality of the fluxes (4.8) and (4.9) as well as for the fact that $H_{1,2} = (\kappa_{1,2}/\omega_r)^{1/2}$, we obtain

$$\omega_r \approx \left(\frac{\kappa_1^{3/2} \rho_{0_1} L_v \alpha_1 g |\gamma_q|}{\kappa_2^{1/2} \rho_{0_2} C_{p_2}} k^2\right)^{1/3}. \tag{4.10}$$

In deriving (4.10), we made a number of simplifying assumptions, and therefore good agreement of (4.10) with (4.1) derived from (3.10) may appear surprising. However, the above-mentioned simplifications can be substantiated sufficiently strictly.

Plotted in figure 6 in the plane of parameters ($\log\omega_r$, $\log L$) are the curves of the increments of growing modes at $\varphi = 1.0$ and $(Ra_1/R_2)\to\infty$, which were calculated numerically from equation (3.10). It is seen from this figure that unstable disturbances of the oscillating type (curves 1, 4) occupy only a rather narrow interval of wavelengths out of the entire range of growing modes. At larger wavelengths, pairs of monotonically growing disturbances remain, which have different ω_r at the same L and therefore different vertical structures. Here it should be noted that in figure 6 just the monotonic

disturbances have the maximum increments, and in the long-wave limit the two-thirds power law ($\omega_r \sim L^{-2/3}$) obtained earlier for a number of anticonvection problems without considering moisture (Ingel & Perestenko 1992) is realized well. There are similar patterns for increments at different values of φ and (Ra_1/R_2), in those situations where oscillatory instability occurs. It may be suggested that a dependence of the form $\omega_r \sim L^{-2/3}$ is common to the instability under consideration.

5. Conclusions

5.1. *Summary*

The main results of the present paper can be formulated as follows.

(i) Within the framework of the linear analysis of stability we investigated the role of moisture in the occurrence of anticonvection in the vicinity of the interface of a water–air system. The key physical parameters of the problem, such as the ratio of the Rayleigh number analogues (Ra_1/R_2) and the density ratio in the moist air φ which determine the position of the stability boundaries of the system in the limit $Ra^{1/3}$, $R_2^{1/3} \gg 1$, were defined.

(ii) A feedback between convective motions in the air and the rate of evaporation from the water surface was found and analysed in detail for the first time. This feedback is enhanced with increasing φ even for stable density stratification of both fluids. The essence of this feedback lies in the fact that a horizontally inhomogeneous thermal disturbance at the interface initiates convective motions in the air and water. Next, the vertical motions arising in the air disturb the vertical moisture profile and hence the magnitude of the latent heat flux from the water surface, thus determining the change of the initial thermal disturbance at the interface. As the magnitude of φ increases, this feedback leads to the disappearance of one of the instability areas for dry anticonvection discovered previously by Gershuni & Zhukhovitsky (1980), Perestenko & Ingel (1989, 1991). It also leads to the appearance of new instability areas, not only of the monotonic type but also of the oscillating type resulting solely from the influence of moisture.

(iii) Using simple physical considerations (see §§3 and 4), we explained a mechanism for the anticonvection development in the monotonic and oscillating regimes, and reproduced the most important asymptotics relating to the stability boundaries and disturbance growth rates. We analysed a physical mechanism for neutral anticonvective oscillations caused by the influence of moisture in the system under study (see §3.4). Such oscillations were shown to exist only at $\varphi \gg \varphi_{min}$. For φ_{min} and the oscillation frequency ω_i we obtained analytically the asymptotic expressions (3.18) and (3.20).

(iv) In §4 we obtained the dependence of the growth rates of unstable disturbances on their wavelengths. The results support the analytical asymptotics which in turn can be illustrated in the simplest cases by descriptive physical considerations (see, for example, (4.1) and (4.10)). The analysis of dispersion curves (see figure 6) shows that although long-wave disturbances have a lower excitation threshold, disturbances in the short-wave range of unstable modes grow most rapidly. Note that oscillating disturbances occupy only a narrow portion of the entire interval of growing modes, with modes of the monotonic type possessing the highest growth rates.

5.2. *Applications*

In discussing, briefly, the applicability of this model and the results obtained to field conditions, it should be emphasized first and foremost, that the formation of the background state tested for stability occurs, as a rule, on the exposure of a cooled water

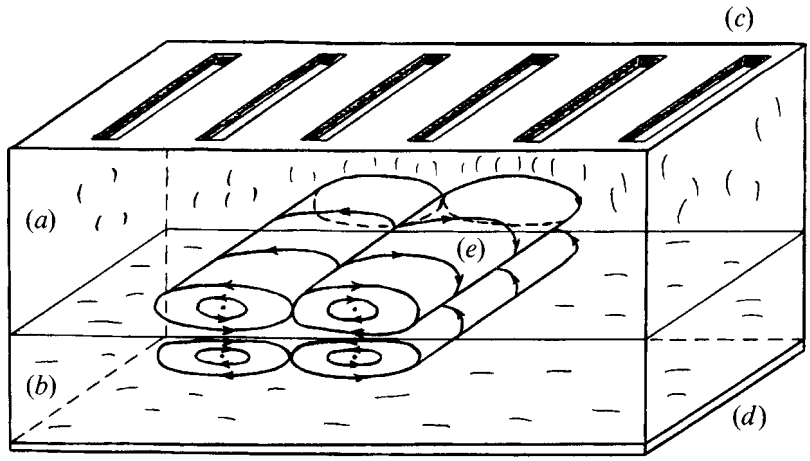

FIGURE 7. A sketch of an experimental installation to be used for observations of moist anticonvection: (*a*) the layer of moist air; (*b*) the layer of tinted water; (*c*) the upper cover, where temperature and moisture are regulated, as well as the location of the source of electromagnetic radiation (a lamp) which enables one to regulate radiation heating of the water surface; (*d*) the lower plate (the bottom), where temperature is regulated; (*e*) a schematic representation of the expected convective cells.

body surface to incoming dry and warm air. This pattern is widespread in coastal regions in the warm season. Also, it is important to note that coastal waters contain a large number of suspended particles, which leads to intensive absorption of short-wave solar radiation in a thin near-surface layer of the water body and the formation of a temperature profile decreasing with depth (the 'warm film' case). If calm conditions are retained for several hours, then temperature and moisture profiles are formed in the interacting laminar layers which are similar to those presented in figure 2, and the conditions occur for realization of an instability of the type considered.

When discussing the applicability of the proposed model to field conditions, we should note that in the present paper the background source of heat Q_R was considered as a free external parameter of the problem. However, in the real ocean–atmosphere system, the radiation balance at the water–air interface determining this source is limited both above and below. Thus, in accordance with the data presented, for example, in the monograph by Matveev (1984), in the warm season the value of Q_R can vary during 24 h from -70 W m^{-2} (at night) to 300 W m^{-2} (by day). It is easy to verify that at different actual values of γ_1 and γ_2 and the above-mentioned range of variation of Q_R, any of the instability regimes investigated in the present paper can be realized in field conditions.

5.3. *Possible laboratory tests*

Being aware of an urgent need to confirm experimentally the phenomenon of anticonvection, we consider now the possibility of observing the investigated instability under laboratory conditions. We believe that this can be done using a specially equipped tank of sufficiently large horizontal dimensions with an upper cover permeable to water vapour (figure 7). When carrying out the experiment, one should regulate both the temperature at the bottom of the tank, and the temperature and moisture of the air at the upper cover. In addition, a source of electromagnetic radiation should be positioned under the upper cover, which will make it possible to regulate horizontally homogeneous radiation heating of the water–air interface. This radiation should be absorbed in a thin near-surface water layer, for which purpose the

water should be tinted with an appropriate admixture. The horizontal dimensions of the tank should be sufficiently large so that the most unstable disturbances will fit in it. By way of example let us consider the possibility of laboratory modelling of anticonvection in the case investigated theoretically in §4. Let the temperature at the bottom of the tank $\bar{T}_b$ be about 30 °C and the water layer depth about 0.1 m. Stratification in the water is regulated through radiation heating of the water surface, so that it will be close to neutral. Then the water surface temperature $\bar{T}_0$ also will be close to about 30 °C, and the corresponding mixing ratio of saturated air $\bar{q}^*$ will be about 3×10^{-2}. Let us assume that the moist air layer depth is about 1 m, and the temperature at the upper cover $\bar{T}_c$ is maintained at about 36 °C, the mixing ratio here being much smaller than that at the water surface. This gives, $\partial_z \bar{q} \sim 3 \times 10^{-2}$ m^{-1}, $\partial_z \bar{T}_1 \sim 6$ K m^{-1}, $\varphi \approx 1$. By regulating the temperature and moisture at the upper cover, one can make the value of φ sufficiently close to unity, i.e. neutral density stratification of the air will be attained. It is evident from the estimated values of heat and moisture fluxes at the water surface that at $\varphi \sim 1$ the inflow of sensible heat from above amounts (in absolute value) to about $\frac{1}{14}$ of the heat outflow at the water surface resulting from evaporation. In the case under consideration, the value of this outflow is about 1.5 wt m^{-2}, and therefore the compensating radiation source of heat at the water–air interface which provides stratification close to neutral in the water layer should be, correspondingly, the same. It follows from the linear analysis of stability performed in §4 that in this case the wavelength of the most rapidly growing mode $L \sim 0.5$ m, whereas disturbances penetrate into the water to the depth $H_2 \sim 5 \times 10^{-2}$ m and into the air to the height $H_1 \sim 0.1$–0.15 m. The respective linear dimensions of the tank should be correspondingly several times larger. In this case the e-folding time is about 10^2 s. The circulation cells that occur can be observed using the conventional techniques employed for studying Rayleigh–Bénard convection.

Appendix. Numerical values of parameters of the fluids

In our calculations we used the following values of the water and air parameters relating to the conditions $T_0 = 293$ K an $\bar{P}_0 = 1.01 \times 10^5$ Pa:

i	1	2
ρ_{0i}(kg m^{-3})	1.18	998.23
C_{pi} (J kg^{-1} K^{-1})	990.7	4.18×10^3
κ_i(m^2 s^{-1})	2.1×10^{-5}	1.43×10^{-7}
ν_i(m^2 s^{-1})	1.5×10^{-5}	1.01×10^{-6}
α_i(K^{-1})	3.4×10^{-3}	2.06×10^{-4}
Pr_i	0.71	7.04

$\sigma_T = 1.44 \times 10^{-4}$ N m^{-1} K^{-1}; $\delta = 0.608$; $L_v = 2.46 \times 10^6$ J kg^{-1}; $\bar{q}^*$ $(\bar{T}_0) = 1.45 \times 10^{-2}$ (kg kg^{-1}); $R_v = 461.5$ J kg^{-1} K. This gives the following values of the dimensionless parameters:

$$\epsilon_1 = 1.76 \times 10^{-2}; \epsilon_2 = 0.90; \quad \epsilon_3 = 3.7 \times 10^{-2}; \quad \epsilon_q = 6.28; \quad \epsilon_L = 13.9.$$

REFERENCES

GERSHUNI, G. Z. & ZHUKHOVITSKY, E. M. 1972 *Convective Stability of an Incompressible Fluid.* Moscow: Nauka.

GERSHUNI, G. Z. & ZHUKHOVITSKY, E. M. 1980 On the instability of equilibrium of a system of horizontal layers of immiscible fluids heated from above. *Izv. Acad. Sci. USSR, Fluid Mech.* **6**, 28–34.

GERSHUNI, G. Z., ZHUKHOVITSKY, E. M. & PERSHINA, E. A. 1983 On the occurrence of convection in some two-layer systems. In *Convective Flows* (*Collection of Scientific Papers of Perm Pedagogical Institute*), pp. 3–24. Perm.

GERSHUNI, G. Z., ZHUKHOVITSKY, E. M. & SIMANOVSKY, I. B. 1981 On the stability of equilibrium and finite-amplitude motions in a two-layer system heated from above. In *Convective Flows* (*Collection of Scientific Papers on Perm Pedagogical Institute*), pp. 3–11. Perm.

INGEL, L. KH. & PERESTENKO, O. V. 1992 On the increments of growing modes in a simple model of the ocean-atmosphere system under the development of the Welander-type instability. *Izv. Acad. Sci. Russia, Atmos. Ocean. Phys.* **28**, 46–54.

INGEL, L. KH. & PERESTENKO, O. V. 1994 A mechanism of intensification of atmospheric convection over a stratified water body. *Met. Hydrol.* **N1**, 12–17.

MATVEEV, L. T. 1984 *The Course of General Meteorology. Physics of the Atmosphere.* Leningrad: Gidrometeoizdat.

NEPOMNYASCHY, A. A. & SIMANOVSKY, I. B. 1990 The occurrence of convection on heating from above and heat release at the interface. *Izv. Acad. Sci. USSR, Fluid Mech.* **N3**, 16–20.

PERESTENKO, O. V. 1992 The occurrence of 'anticonvection' in two-layer fluids in the presence of thermocapillary effects. *Lett. J. Thechn. Phys.* **18** (20), 5–10.

PERESTENKO, O. V. 1993 Occurrence of convective instability in the interacting stably stratified layers of the ocean and atmosphere. Dissertation thesis, Institute of Experimental Meteorology, Obninsk, 210 pp.

PERESTENKO, O. V. & INGEL, L. KH. 1989 On the possibility of the Welander-type instability in the ocean-atmosphere system. *Tropical Meteorology. Proc. 4th Intl Symp*, pp. 299–311. Leningrad: Gidrometeoizdat.

PERESTENKO, O. V. & INGEL, L. KH. 1991 On one possible type of convective instability in the ocean-atmosphere system. *Izv. Acad. Sci. USSR, Atmos. Ocean. Phys.* **27**, 408–418.

PERESTENKO, O. V. & INGEL, L. KH. 1993 On a mechanism of instability of a stably stratified atmospheric boundary layer over a moistened underlying surface. *Dokl. Akad. Nauk Russia* **333**, **N1**, 92–95.

STERNLING, C. V. & SCRIVEN, L. E. 1959 Interfacial turbulence: hydrodynamic instability and the Marangoni effect. *AIChE J.* **5**, 514–523.

WELANDER, P. 1964 Convective instability in a two-layer fluid heated uniformly from above. *Tellus* **16**, 349–358.

WELANDER, P. 1971 Instability due to heat diffusion in a stably stratified fluid. *J. Fluid Mech.* **47**, 51–64.